

Molecular Docking of Ecdysone Agonists and Limonoid Components of Calamondin Seeds to Tobacco Budworm Ecdysone Receptor

Annabelle T. Abrera^{1,2}, Melvin A. Castrosanto², Joseph Anthony C. Hermocilla^{1,3}, Marlon N. Manalo^{1,2*}

¹ Computational Interdisciplinary Research Laboratories, University of the Philippines Los Baños, College, Laguna 4031

² Institute of Chemistry, University of the Philippines Los Baños, College, Laguna 4031

³ Institute of Computer Science, University of the Philippines Los Baños, College, Laguna 4031

*Author to whom correspondence should be addressed; email: mnmanalo@up.edu.ph

ABSTRACT

Molecular docking of calamondin limonoids to tobacco budworm ecdysone receptor was performed to calculate binding affinities and evaluate their potential as an insecticide. Results were compared to those of 20-hydroxyecdysone, ponasterone A, and known ecdysone agonists by examination of binding interactions between the ligands and receptor. While an earlier study by other researchers attributed the stronger binding of ponasterone A to (de)solvation effects, molecular dynamics simulations in this study revealed stronger hydrogen bonds between the receptor and ponasterone A, consistent with calculated binding affinities from molecular docking. None of the limonoids and ecdysone agonists showed stronger binding affinity than 20-hydroxyecdysone, suggesting that site-specific docking may not be suitable to predict the binding interactions of these non-steroidal ligands with tobacco budworm ecdysone receptor. The computational approach described in this study can be used in the preliminary screening of compounds for bioactivity against receptors with known active sites.

Keywords: *ecdysone receptor; limonoid; tobacco budworm*

INTRODUCTION

Due to the persistence and harmful effects of several insecticides available in the market, many studies are now focused on developing environmentally benign insecticides. One such group of compounds that have been reported to have potent effects on insects and low toxicity to non-target organisms are limonoids (Abdelgaleil and El-Aswad, 2005). Limonoids are the prominent secondary metabolite present in citrus and are responsible for the bitter taste in juice. Limonoids are described as modified triterpenes derived from a precursor with a 4,4,8-trimethyl-17-

furanylsteroid skeleton. Over 300 limonoids have been isolated to date and they are found in citrus in three major forms: limonoid dilactones, limonoid monolactones, and limonoid glucosides (Manners, 2007).

Limonoids are known to have a wide range of biological activities, including insect anti-feedant, anti-oxidant, anti-fungal, anti-bacterial, anti-viral, anti-carcinogenic, and growth-inhibiting characteristics. In a study conducted by Dinan et al. (1997), limonoids and other plant natural products were found to antagonize the action of 20-hydroxyecdysone (20E, Figure 1). Juvenile hormones and 20E are the major hormones that regulate ecdysis (insect molting), which is controlled by activation of ecdysone receptor (EcR) through binding of 20E. Binding of agonists blocks the activity of ecdysone hormone and prevents molting, thus breaking the life cycle of the insect (Laguerre and Veenstra, 2010). Several compounds acting as ecdysone agonists are already available in the market. These compounds are dibenzoylhydrazine (DBH) analogues (Nakagawa, 2007), also called diacylhydrazines (Sparks and Nauen, 2015), and include tebufenozide, chromafenozide, and methoxyfenozide (Figure 2).

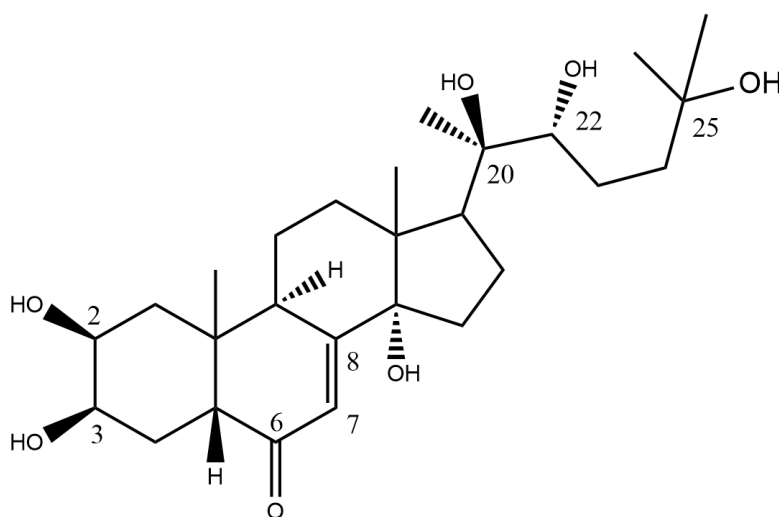


Figure 1. Chemical structure of 20E with numerical labels in the important structural features used in this study.

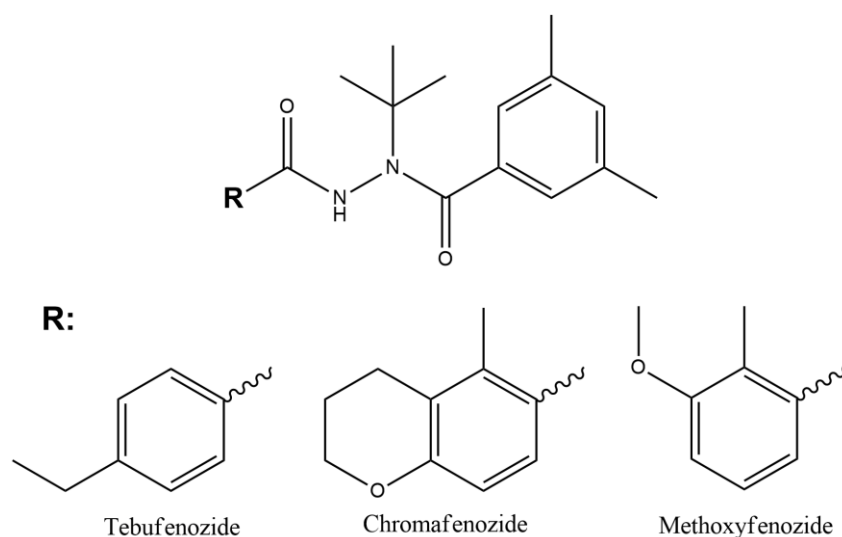


Figure 2. Chemical structures of the diacylhydrazine ligands used in site-specific docking.

Kasuya et al. (2003) constructed two three-dimensional structure models of the ligand-binding domain of the EcR of *Heliothis virescens* (tobacco budworm) based on known ligand-binding domain structures of the receptors with the highest sequence identity to the EcR and steroid hormone receptors. They illustrated the binding of 20E and chromafenozide on EcR using molecular modeling and virtual docking. A few years later, Browning et al. (2007) reported the crystal structure of the ligand-binding domains of EcR/ultraspiracle (USP) with co-crystallized 20E at 2.402 Å resolution and compared it with published structures of EcR/USP bound to ponasterone A (ponA), an analog of 20E. Results of their docking calculations, however, showed stronger binding of 20E than ponA, which contradict experimental data.

In a study by Yadav et al. (2015), *in silico* docking of non-azadirachtin neem limonoids against EcR of *Helicoverpa armigera* was used to screen for potential agonists. A similar approach was employed in the present study to evaluate the binding affinity of calamondin limonoids to the EcR/USP crystal structure reported by Browning et al. (2007). Limonoids from seeds of calamondin (*Citrus reticulata* var. *austera* × *Fortunella* sp.) have been isolated by Miyake et al. (1992), which include nomilinic acid, deacetylnomilinic acid, methyl deacetylnomilinate, 6-keto-7β-deacetylnomilol, and calamin (Figure 3). Site-specific docking of these five limonoids to tobacco budworm EcR/USP was performed in this study and results were compared against those of the natural ligand 20E and the diacylhydrazines mentioned above. Our objective was to determine if any of these known limonoids would have a higher binding affinity than 20E, which could potentially make them useful as an insecticide. Since calamondin is a close relative of calamansi [*Citrofortunella microcarpa* (Bunge) Wijnands], the limonoids that would show significant binding to EcR/USP may also be present in calamansi, thereby making the latter a potentially abundant source of these natural insecticides.

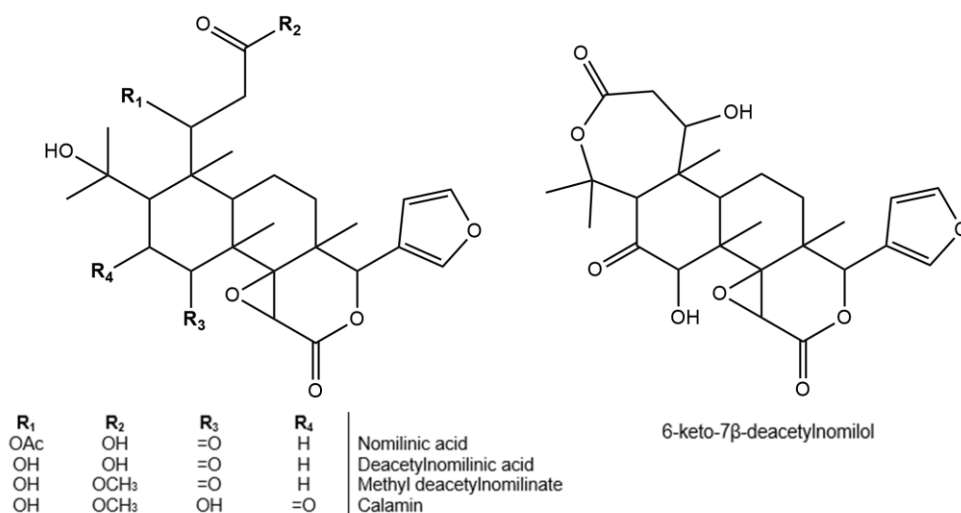


Figure 3. Chemical structures of the calamondin limonoids used in site-specific docking.

METHODS

Preparation of the Receptor Model. The crystal structure of 20E-bound EcR/USP of *Heliothis virescens* (Browning et al., 2007) was obtained from Protein Data Bank (PDB ID: 2R40). This structure consists of two main polypeptide chains (EcR and USP), five “ligand” components including 20E, and solvent water molecules. To generate the receptor structure used in virtual docking, all solvent molecules and ligands were deleted using Avogadro (Hanwell et al., 2012). Hydrogen atoms were then added using Avogadro’s “Add Hydrogens” function, and the structure was saved as a new pdb file.

Preparation of the Ligand Models. Calculations were carried out on a VirtualBox virtual machine running Windows 10 (1809) and Gaussian 09W (Frisch et al., 2010). The host machine is a 32-core Intel(R) Xeon(R) CPU E5-2618L v3 @ 2.30 GHz with 94 GB RAM and 2.7 TB hard disk storage. The virtual machine was allocated 16 cores and 12 GB RAM, of which 12 cores and 6 GB were used for the actual Gaussian runs. Geometry optimization of 20E was performed using Hartree-Fock (HF) and density functional theory (DFT) methods. The minimal basis set STO-3G was used for the HF calculation, whereas variations of the Pople basis set 6-31G were used for the DFT calculations using the B3LYP functional. The resulting structures were then compared against that of the experimental (co-crystallized) 20E to determine the method that would yield the lowest root-mean-square deviation (RMSD). This method was then used for geometry optimization of ponA and its derivatives, chromafenozide, methoxyfenozide, tebufenozide, and the five calamondin limonoid aglycones. The structure of ponA is similar to 20E (Figure 1) but lacking the 25-OH group. PonA derivatives used in this study include ponA-ketone (saturated at C7 and C8), ponA-enol (-OH at C6, with C6-C7 double bond), ponA-eqOH (saturated at C7 and C8, with equatorial -OH at C6), and ponA-axOH (saturated at C7 and C8, with axial -OH at C6).

Virtual Docking. The binding of ligands to the receptor was investigated *in silico* with AutoDock Vina (Trott and Olson, 2010) through the user interface of PyRx 0.8 (Dallakyan and Olson, 2015). The size of the search space was 12.2209 Å x 18.5549 Å x 17.2069 Å, which was centered at the following coordinates: x = 24.9857, y = -4.5515, z = -6.1031. Exhaustiveness was set to the default value of 8. To validate the docking parameters, the experimental structure of 20E was generated from 2R40 by deleting all components except the co-crystallized 20E. Hydrogen atoms were then added using Avogadro's "Add Hydrogens" function. This experimental 20E structure was then "re-docked" to the receptor model, and its RMSD against the original co-crystallized 20E was calculated. After validating the docking parameters, the geometry-optimized ligands were docked to the ECR/USP receptor using the same set of parameters. Binding interactions were analyzed using Discovery Studio (BIOVIA, Dassault Systèmes).

Molecular Dynamics. Molecular dynamics (MD) simulations have been widely used to gain insights into the structural dynamics of biomolecular systems (Meelua et al., 2021). To obtain the thermally equilibrated system of 2R40-20E and 2R40-ponA, each complex was subjected to 20-ns MD simulation using Desmond (Bowers et al., 2007). The complexes were solvated with water molecules using the SPC model in the Desmond System Builder tool. An orthorhombic simulation box shape with dimensions of 4.0 Å x 4.0 Å x 10.0 Å was generated. The system was neutralized by adding Na⁺ and Cl⁻ and 0.15 M salt concentration to conserve isosmotic condition. The simulation (NPT) was set to 20 ns with a recording interval of 20 ps at 300 K and 1.01325 bar. The structural and dynamic properties were obtained by analyzing the RMSD and the ligand interactions throughout the simulation.

RESULTS AND DISCUSSION

To test the binding of the ligands to EcR computationally, it was necessary to perform geometry optimization of the structure of these compounds. Highly accurate ligand structures are, however, not necessary for virtual screening since docking generally assumes that the receptor is rigid (Trott and Olson, 2010). For this reason, geometry optimizations were carried out using only small basis sets. Geometry optimizations were tested using HF and DFT, while adjusting the basis set accordingly. The goal was to obtain an optimized structure for 20E that would give a low RMSD (heavy atoms only) when compared against the experimental (co-crystallized) 20E structure. Initial geometry optimization of 20E using HF/STO-3G gave an RMSD of 2.112 Å, which is already within the resolution of the crystal structure. To improve the optimization, DFT was employed, specifically the B3LYP method coupled with 6-31G(d) basis set, resulting in a slightly lower RMSD of 2.105 Å. The addition of polarization function to the hydrogen atoms of 20E using the basis set

6-31G(d,p) raised the RMSD to 2.572 Å, which is higher than the experimental resolution. Inclusion of diffuse function to the heavy atoms via the 6-31+G(d) basis set also resulted in a higher RMSD of 2.111 Å. Thus, basis sets with diffuse functions added to the heavy atoms or polarization functions added to the hydrogen atoms were not considered. Lastly, geometry optimization of 20E was performed using the triple split valence basis set 6-311G(d), which yielded an RMSD of 1.889 Å. Since this value is significantly lower than the resolution of the experimental structure, geometry optimization of all the ligand structures were carried out at the B3LYP/6-311G(d) level.

Validation of the docking parameters is an important first step in the theoretical evaluation of the binding of candidate ligands to a target receptor. An easy, but effective way of achieving this is to take an experimentally determined structure of the native ligand-receptor complex, separate the ligand and receptor macromolecule, and then apply the docking program to allow the ligand to “re-dock” to the receptor. This simple test was applied to evaluate the docking parameters used in calculating binding affinities. The low RMSD of 0.354 Å between the co-crystallized 20E and re-docked 20E indicates that our docking parameters are reasonable for calculating binding affinities (Figure 4).

Table 1 lists the binding affinities of the EcR/USP-ligand complexes for the geometry-optimized 20E, ponA, and ponA derivatives. Note that a more negative value for binding affinity indicates a more stable complex, and therefore stronger binding of the ligand to the receptor. Our docking results show that the binding of 20E to the receptor is weaker than that of ponA, which is consistent with biological data (Dhadialla et al., 1998). In comparison, the docking results of Browning et al. (2007) predicted better binding of 20E over ponA. Consequently, they suggested that important effects were poorly treated in their models, particularly (de)solvation effects.

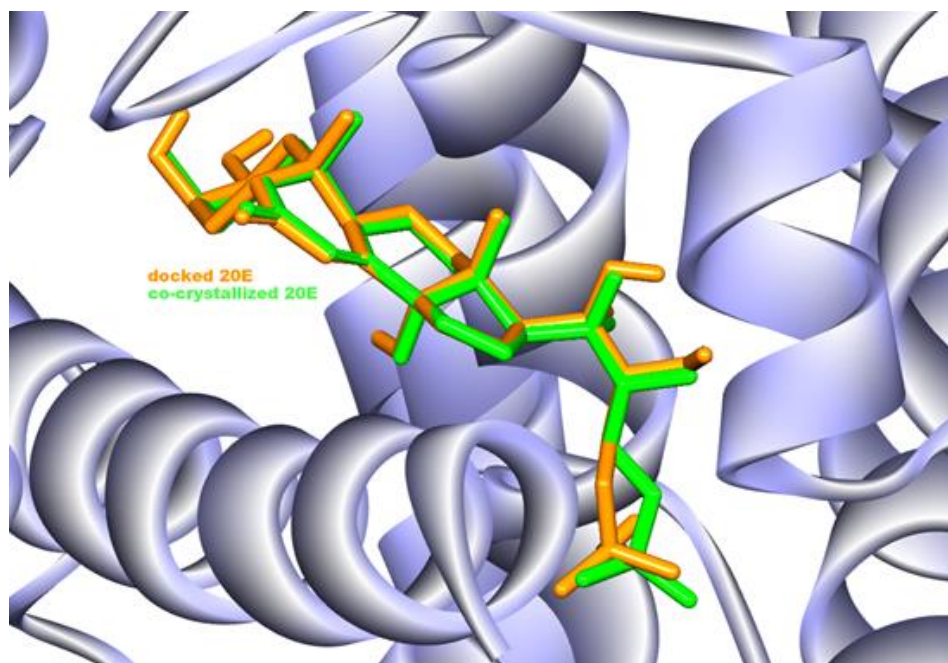


Figure 4. Superimposition of the co-crystallized 20E (orange) and the re-docked 20E (green), with RMSD of 0.354 Å.

Table 1. Binding affinities of the most stable complex predicted by molecular docking of 20E, ponA, and ponA derivatives.

Ligand	Binding affinity / kJ mol ⁻¹
20E	-35.1
ponA	-50.2
ponA-ketone	-49.8
ponA-enol	-48.5
ponA-eqOH	-49.0
ponA-axOH	-45.2

The stronger binding affinity of ponA can be mostly accounted for by its additional binding interactions, which are correspondingly absent in 20E. These include H-bonding with E309 and alkyl interactions with I339 and M413 (Figure 5). On the other hand, the 25-OH group of 20E, which is absent in ponA, does not show any detectable conventional H-bonding interaction and therefore contributes insignificantly to the calculated binding affinity. The carbonyl oxygen of both 20E and ponA form H-bond with the backbone amino hydrogen of A398. This H-bond, however, is much weaker for 20E due to the longer donor-acceptor distance (Table 2). This could explain the significant difference in binding affinity between 20E and ponA, in addition to the (de)solvation effects suggested by Browning et al. (2007). The significant contribution of H-bonding interaction with A398 to the binding affinity is further supported by the higher binding affinities of the ponA derivatives (Table 1), which also show shorter H-bond donor-acceptor distances compared with 20E (Table 2).

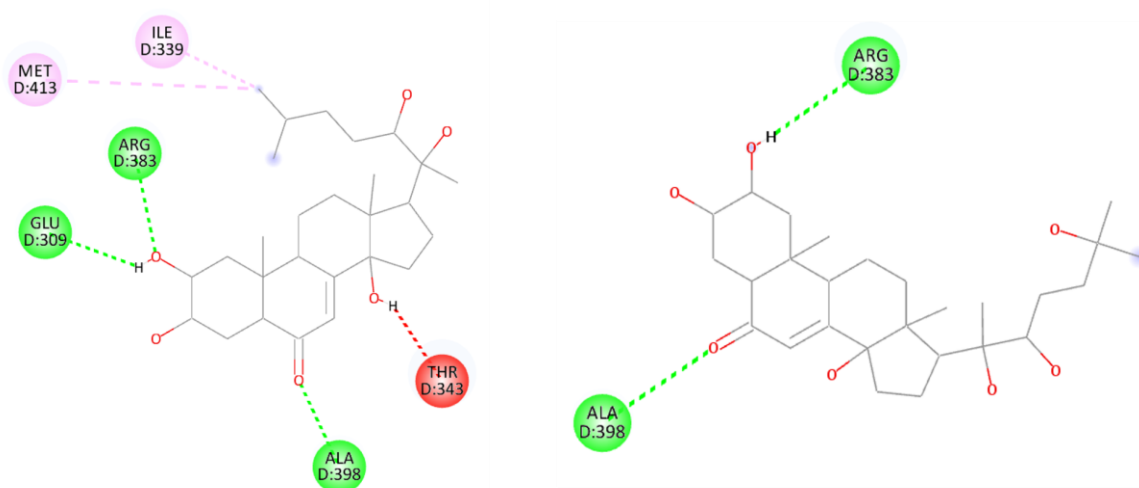


Figure 5. The 2D interaction diagram of 2R40 with ponA (left) and 20E (right) showing conventional H-bonds (green), hydrophobic interactions (pink), and unfavorable H-bonds (red).

Table 2. Distances and angles for the H-bond between A398 backbone N-H and the corresponding acceptor O of 20E, ponA, and ponA derivatives.

Ligand	NH—O distance / Å	N—H—O angle / deg
20E	2.724	150.42
ponA	1.855	163.86
ponA-ketone	1.741	169.05
ponA-enol	1.984	173.08
ponA-eqOH	1.847	173.48
ponA-axOH	2.103	147.45

To determine other possible H-bonding interactions not detected by site-specific docking in Autodock Vina, MD simulations of binding of 20E and ponA to the EcR/USP receptor were performed. Although these interactions do not account for the binding affinity values reported in Table 1, they can further explain the higher affinity of ponA to the receptor, compared to that of 20E. Figure 6 shows the H-bonds predicted by MD simulations and the percentage of simulation time in the selected trajectory (0 to 20 ns) that they occurred. For ponA, the significant ligand: protein H-bonds include 2-OH: R383 (101%, indicating multiple H-bond sites on R383), 6-CO: A398 (100%), and 20-OH: Y408 (94%), which are consistent with those reported by Billas et al. (2003). For 20E, the MD simulations did not detect any H-bonds with R383. In addition, Y408 was found to interact with 14-OH of 20E instead of 20-OH as seen in ponA. Although the 25-OH of 20E (which is absent in ponA) have interactions with T343 and N504, these occurred in no more than 25% of the simulation time. Moreover, ponA also has interactions with these residues in other sites of the molecule. It can also be seen in Figure 6 that there is an intramolecular H-bond in 20E between the carbonyl oxygen on C6 and 3-OH. This could account for the weaker H-bond between the backbone amino hydrogen of A398 and 20E compared to that of ponA, as mentioned above. The MD simulations generally predict more consistent and stronger H-bonds for ponA, some of which are not detectable in the site-specific docking with Vina. The 20-ns simulation time was determined to be sufficient for investigating the protein-ligand contacts because the complexes remained stable and equilibrated, as indicated by the low protein and ligand RMSD ($< 2 \text{ \AA}$), over the course of the simulation (Figure 7).

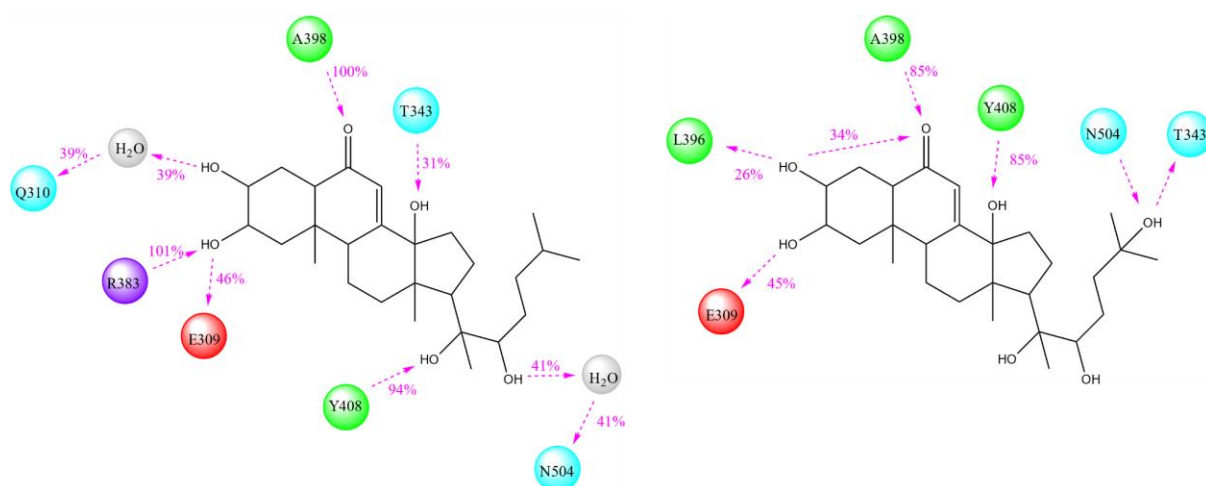


Figure 6. The H-bonds present in the 2R40 complex with ponA (left) and 20E (right) resulting from the 20-ns MD simulation. Percentages of the interaction occurrence over the course of simulation are shown along with the amino acid residues involved. The colors depict the nature of the residues (green, hydrophobic; blue, polar; purple, positively charged; red, negatively charged).

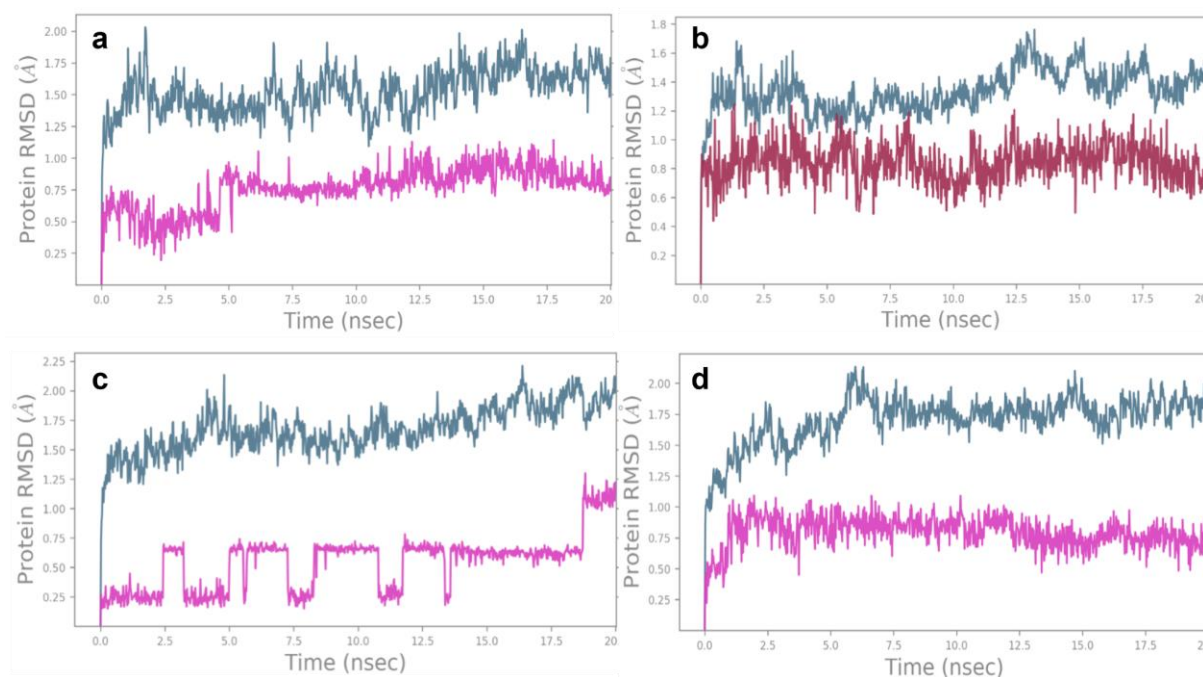


Figure 7. Protein-ligand RMSD plots of the 20-ns MD simulation for 20E (a), ponA (b), 6-keto-7 β -deacetylnomilol (c), and chromafenozide (d). For each plot, the top curve shows the RMSD evolution of the protein, and the bottom curve shows the RMSD evolution of the ligand atoms.

Compared with 20E, all of the limonoids used in this study were found to have weaker binding to the receptor. Among them, 6-keto-7 β -deacetylnomilol showed the strongest binding (Table 3) due to the presence of H-bond interactions with R383 and A398. Ligand contacts with the same protein residues are also responsible for the calculated binding affinity of 20E, although they are weaker for the limonoid due to the longer H-bond distances. Nomilinic acid, on the other hand, does not have interactions with these residues. Methyl deacetylnomilinate has H-bonds with A398 and T346, but these are offset by the unfavorable steric and repulsive contacts with Y408 and T343, respectively. Calamin also has unfavorable steric contact with Y408 despite having H-bond interactions with I339, T346, and R383. Deacetylnomilinic acid showed the weakest binding among the limonoids calculated due to the same unfavorable contacts found in methyl deacetylnomilinate and calamin. The binding affinities calculated for the diacylhydrazines are also less negative compared to that obtained for 20E, primarily due to the absence of strong contacts with the receptor in the site-specific docking calculations. Most ligand-protein contacts found in these compounds when they are restricted to the same binding site as 20E are hydrophobic, such as alkyl and π -alkyl interactions.

Table 3. Binding affinities calculated for the most stable complex predicted by molecular docking of calamondin limonoids and DBH compounds.

Ligand	Binding affinity / kJ mol ⁻¹
deacetylnomilinic acid	-16.3
methyl deacetylnomilinate	-24.7
calamin	-22.6
6-keto-7 β -deacetylnomilol	-26.4
nomilinic acid	-25.5
chromafenozide	-33.9
methoxyfenozide	-8.8
tebufenozide	-31.4

Based on the calculated binding energies from site-specific docking, all of the limonoids and DBH compounds used in this study have weaker binding to EcR than the natural ligand 20E. Thus, MD simulations were performed only for the top limonoid and DBH compound. Figure 8 shows that the H-bonding interactions of 6-keto-7 β -deacetylnomilol are through water molecule bridges only and not direct H-bonding with the receptor residues. Moreover, the observed H-bonding with A398 in the site-specific docking is not detected in the MD simulation. For chromafenozide, one direct H-bonding interaction is present between the ligand and N504. This is far less than the H-bonding interactions present in the MD simulation of 20E (Figure 6). Since diacylhydrazines are known to effectively disrupt molting in lepidopterous insect pests by mimicking the action of 20E, it is likely that site-specific molecular docking was not able to predict their correct binding poses resulting in low binding affinities. As reported by Billas et al. (2003), the ligand-binding domain of tobacco budworm EcR can adopt different binding cavities. Thus, it is recommended to perform flexible or blind docking when investigating the binding of ligands, such as limonoids, to the tobacco budworm EcR.

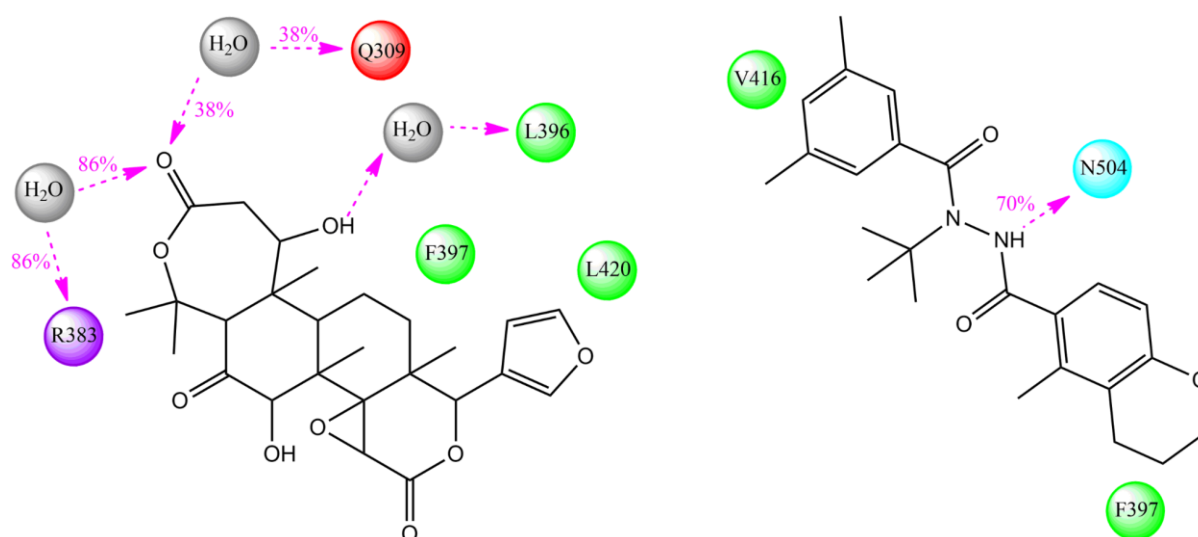


Figure 8. The H-bonds present in the 2R40 complex with 6-keto-7 β -deacetylnomilol (left) and chromafenozide (right) resulting from the 20-ns MD simulation. Percentages of the interaction occurrence over the course of simulation are shown along with the amino acid residues involved. The colors depict the nature of the residues (green, hydrophobic; blue, polar; purple, positively charged; red, negatively charged).

CONCLUSIONS

This study aimed to screen limonoids in calamondin for potential insecticidal activity by calculating their binding affinities to EcR using molecular docking. Site-specific docking using AutoDock Vina was able to predict the higher affinity of ponA to EcR compared with 20E, despite the absence of 25-OH in ponA. Measurement of hydrogen bond distances suggests that the interaction between residue A398 of the receptor and C6-carbonyl oxygen of ponA is stronger than that of 20E. This is supported by the molecular dynamics simulations that revealed more consistent and stronger H-bonds for ponA, which contribute to its stronger binding to EcR. Although site-specific docking was able to explain the conundrum of ponA/20E binding affinity, its results showed weaker binding for the known ecdysone agonists when compared against 20E. This indicates that the binding site of these ligands may not be identical to that of 20E since the ligand-binding pocket of EcR is known to be highly flexible and ligand-dependent. Site-specific docking also indicated weaker binding of the limonoids to EcR, suggesting the possibility of

binding modes that are not identical to that of 20E. Thus, it is recommended to use blind docking in calculating the binding affinities of such non-steroidal ligands in order to evaluate their potential insecticidal activity.

REFERENCES

Abdelgaleil SAM, El-Aswad AF. Antifeedant and growth inhibitory effects of tetranortriterpenoids isolated from three Meliaceae species on the cotton leafworm, *Spodoptera littoralis* (Boisd.). J Appl Sci Res. 2005 Jan; 1(2):234-241. <http://www.aensiweb.com/old/jasr/jasr/234-241.pdf>

Billas IML, Iwema T, Garnier JM, Mitschler A, Rochel N, Moras D. Structural adaptability in the ligand-binding pocket of the ecdysone hormone receptor. Nature. 2003 Nov; 426:91-96. <https://doi.org/10.1038/nature02112>

BIOVIA Discovery Studio v21.1.0.20298, San Diego: Dassault Systèmes, 2021. <https://www.3ds.com/products-services/biovia/products/molecular-modeling-simulation/biovia-discovery-studio>

Bowers KJ, Chow E, Xu H, Dror RO, Eastwood MP, Gregersen BA, et al. Scalable algorithms for molecular dynamics simulations on commodity clusters. Proceedings of the ACM/IEEE Conference on Supercomputing (SC06). 2006 Nov 11-17; Tampa, Florida. <https://doi.org/10.1145/1188455.1188544>

Browning C, Martin E, Loch C, Wurtz J, Moras D, Stote RH, et al. Critical role of desolvation in the binding of 20-hydroxyecdysone to the ecdysone receptor. J Biol Chem. 2007 Nov; 282(45):32924-32934. <https://doi.org/10.1074/jbc.M705559200>

Dallakyan S, Olson AJ. Small-molecule library screening by docking with PyRx. In: Hempel J, Williams C, Hong C, editors. Chemical biology. Methods in Molecular biology, vol 1263. New York, NY: Humana Press; 2015. p. 243-250. https://doi.org/10.1007/978-1-4939-2269-7_19

Dhadialla TS, Carlson GR, Le DP. New insecticides with ecdysteroidal and juvenile hormone activity. Annu Rev Entomol. 1998 Jan; 43:545-569. <https://doi.org/10.1146/annurev.ento.43.1.545>

Dinan L, Whiting P, Girault JP, Lafont R, Dhadialla TS, Cress DE, et al. Cucurbitacins are insect steroid hormone antagonists acting at the ecdysteroid receptor. Biochem J. 1997 Dec; 327(3):643-650. <https://doi.org/10.1042/bj3270643>

Frisch MJ, Trucks GW, Schlegel HB, Scuseria GE, Robb MA, Cheeseman JR, et al. Gaussian 09, Revision C.01. Gaussian, Inc., Wallingford CT; 2010. <https://gaussian.com/g09citation>

Hanwell MD, Curtis DE, Lonie DC, Vandermeersch T, Zurek E, Hutchison GR. Avogadro: An advanced semantic chemical editor, visualization, and analysis platform. J. Cheminformatics. 2012 Aug; 4(17): 1-17. <http://www.jcheminf.com/content/pdf/1758-2946-4-17.pdf>

Kasuya A, Sawada Y, Tsukamoto Y, Tanaka K, Toya T, Yanagi M. Binding mode of ecdysone agonists to the receptor: comparative modeling and docking studies. J Mol Model. 2003 Feb; 9(1):58-65. <https://doi.org/10.1007/s00894-002-0113-x>

Laguerre M, Veenstra JA. Ecdysone receptor homologs from mollusks, leeches and a polychaete worm. FEBS Letters. 2010 Nov; 584(21):4458-4462. <https://doi.org/10.1016/j.febslet.2010.10.004>

Manners GD. Citrus limonoids: analysis, bioactivity, and biomedical prospects. *J Agric Food Chem*. 2007 Oct; 55(21):8285–8294. <https://doi.org/10.1021/jf071797h>

Meelua W, Wanjai T, Thinkumrob N, Olah J, Mujika JI, Ketudat-Cairns JR, et al. Active site dynamics and catalytic mechanism in arabinan hydrolysis catalyzed by GH43 endo-arabinanase from QM/MM molecular dynamics simulation and potential energy surface. *J Biomol Struct Dyn*. 2021 Mar; 1(11). <https://doi.org/10.1080/07391102.2021.1898469>

Miyake M, Ozaki Y, Ayano S, Bennett RD, Herman Z, Hasegawa S. Limonoid glucosides in calamondin seeds. *Phytochemistry*. 1992 Mar; 31(3):1044-1046. [https://doi.org/10.1016/0031-9422\(92\)80070-U](https://doi.org/10.1016/0031-9422(92)80070-U)

Nakagawa Y. Structure–activity relationship and mode of action study of insect growth regulators. *J Pestic Sci*. 2007 Feb; 32(2):135–136. <https://doi.org/10.1584/jpestics.J07-01>

Sparks TC, Nauen R. IRAC: Mode of action classification and insecticide resistance management. *Pestic Biochem Phys*. 2015 Jun; 121: 122-128. <https://doi.org/10.1016/j.pestbp.2014.11.014>

Trott O, Olson AJ. AutoDock Vina: improving the speed and accuracy of docking with a new scoring function, efficient optimization and multithreading. *J Comput Chem*. 2010 Jan; 31(2):455-461. <https://doi.org/10.1002/jcc.21334>

Yadav RP, Syed Ibrahim K, Gurusubramanian G, Senthil Kumar N. *In silico* docking studies of non-azadirachtin limonoids against ecdysone receptor of *Helicoverpa armigera* (Hubner) (Lepidoptera: Noctuidae). *Med Chem Res*. 2015 Jan; 24:2621–2631. <https://doi.org/10.1007/s00044-015-1320-1>